Structural Evolution of Tensile-Deformed High-Density Polyethylene during Annealing: Scanning Synchrotron Small-Angle X-ray Scattering Study

8 AUTHORS, INCLUDING:

Yongfeng Men
Chinese Academy of Sciences
86 PUBLICATIONS   1,405 CITATIONS

Stephan V Roth
Deutsches Elektronen-Synchrotron
363 PUBLICATIONS   3,262 CITATIONS

Rainer Gehrke
Deutsches Elektronen-Synchrotron
170 PUBLICATIONS   1,572 CITATIONS

Jens Rieger
Harvard University
55 PUBLICATIONS   1,739 CITATIONS

Structural Evolution of Tensile-Deformed High-Density Polyethylene during Annealing: Scanning Synchrotron Small-Angle X-ray Scattering Study

Zhiyong Jiang,[†] Yujing Tang,[†] Yongfeng Men,*,[†] Hans-Friedrich Enderle,[‡] Dieter Lilge,[‡] Stephan V. Roth,[§] Rainer Gehrke,[§] and Jens Rieger[||]

State Key Laboratory of Polymer Physics and Chemistry, Changchun Institute of Applied Chemistry, Chinese Academy of Sciences, Graduate School of Chinese Academy of Sciences, Renmin Street 5625, 130022 Changchun, P.R. China, Basell Polyolefine GmbH, R&D, 65926 Frankfurt, Germany, HASYLAB am DESY, Notkestr. 85, 22607 Hamburg, Germany, and BASF Aktiengesellschaft, Polymer Physics, 67056 Ludwigshafen, Germany

ABSTRACT: The structural evolution of high-density polyethylene subjected to uniaxial tensile deformation was investigated as a function of strain and after annealing at different temperatures using a scanning synchrotron small-angle X-ray scattering (SAXS) technique. The results confirm that in the course of tensile deformation intralamellar block slips were activated at small deformations followed by a stress-induced fragmentation and recrystallization process yielding thinner lamellae with their normal parallel to the stretching direction. The original sheared lamellae underwent severe internal deformation so that they were even less stable than the newly developed thinner lamellae. Accordingly, annealing results in a melting of the original crystallites even at moderate strains where the stress-induced fragmentation and recrystallization just sets in and generates a distinctly different form of lamellar stacks aligned along the drawing direction. It was found that the lamellae newly formed during stretching at moderate strains remain stable at lower temperature. Only at a very high annealing temperature of 120 °C can they be melted, leading to an isotropic distribution of the lamellar structure.

1. Introduction

High-density polyethylene (HDPE) is the simplest polymer with respect to its chemical structure and used in a wide range of fields, such as distribution pipes for water, gas, and oil, high-strength fibers, and containers. All these applications are based on the well-balanced mechanical performance of solid HDPE that includes its modulus, chemical and mechanical fracture resistance, etc. To a large extent, the mechanical properties of HDPE depend on its microstructure and morphology.[1−4] After solidification, polyethylene, like many other crystallizable polymers, crystallizes into periodically stacked lamellar crystals with amorphous polymeric chains in between forming the so-called semicrystalline state.[5] The interconnected hard crystalline phase provides rigidity for the system, whereas the soft amorphous phase toughens the material.[6,7] It is essential to study the microstructural changes during mechanical treatments of the material in order to gain more insight into the molecular mechanisms of deformation and thus provide possible routes for improvement of the material.[7−15] Two general but distinctly different arguments about the tensile deformation mechanism of semicrystalline polymers have been proposed in the literature. First, it was suggested that deformation is accomplished by slips within the lamellae including crystallographic fine slips and intralamellar mosaic block slips;[16−21] second, stress-induced melting and recrystallization was proposed to be responsible for the variation of morphology in the deformation process.[22,23] Experimental evidence for both arguments have been extensively

reported including microscopic and X-ray diffraction investigations supporting the slip mechanism[17,20,24] and small-angle X-ray scattering (SAXS) experiments favoring the melting−recrystallization scheme.[25−27] In recent years, investigations based on "true stress−strain experiments" reveal that both processes discussed above are activated in the course of tensile deformation of semicrystalline polymers.[6,12,28] Upon stretching, block slippage within the crystalline lamellae takes place first, followed by the stress-induced fragmentation and recrystallization of the polymeric chains at larger deformation. It was also found that the onset of the stress-induced fragmentation and recrystallization process depends on the entanglement state of the amorphous phase and the stability of the crystalline blocks.[7] In the case of polyethylene, a critical true strain of about 0.6 for this onset point was obtained.[28] The tensile deformation transforms the originally macroscopically isotropic semicrystalline polymers into a highly oriented fibrous material with polymeric chains preferentially aligned along the drawing direction. This evolution of the microstructure was assumed to proceed via fragmentation and recrystallization and can be evidenced directly with the SAXS technique in the bulk state without special sample preparation procedures.[8,29−31] On the other hand, Galeski et al. claimed that this process can be explained on the grounds of crystallographic mechanisms alone;[21] see also ref 20, 32, and 33. According to this approach the plastic deformation initially proceeds primarily by fine chain slip, which leads to reorientation of both chain direction and lamella normal and, consequently, substantial thinning of lamellae and reduction of the long period. Such thinning leads to slip instabilities and then to heavy fragmentation of lamellae into small crystalline blocks. Now, these blocks become free of constraints imposed previously upon the lamellae and can not only rotate to produce a new long period along the drawing

* To whom correspondence should be addressed. E-mail: men@ciac.jl.cn.
† Chinese Academy of Sciences.
‡ Basell Polyolefine GmbH.
§ HASYLAB am DESY.
|| BASF Aktiengesellschaft.

direction but also reshape to reduce the interface energy. The latter leads to an increase in the thicknesses of the lamellae thinned in the previous step, up to that characteristic just for the actual temperature.

In real-life applications one often meets situations where a product is used under varying temperature conditions. Moreover, many procedures used in industry to determine the lifetime of the final products are conducted at elevated temperatures.[34] In such a case, knowledge about the changes of microstructure, both in the initial isotropic state and in the oriented one, upon annealing is important.[35-38] In the present work, we study the microstructural evolution of HDPE at different deformation ratios after subsequently annealing at different temperatures by means of synchrotron SAXS. As will be shown in the following sections, SAXS results first of all confirm the occurrence of both deformation mechanisms discussed above: a transition from slip processes to fragmentation and recrystallization at a certain strain is deduced from 2-D SAXS patterns. It was also found that annealing the samples at elevated temperatures is accompanied by several structural effects on the nanometer scale depending on the temperature of annealing. Furthermore, the strongest influence of annealing on the microstructure is found at moderate strains after the onset of the stress-induced fragmentation and recrystallization process. It must be stressed that data treatment is performed in a semiquantitative manner, mainly relying on the interpretation of changes observed in the scattering patterns upon variation of the experimental parameters, temperature of annealing, and strain. No effort is undertaken to give a complete description of the data by fitting a structural model to the data because still too many structural details of the material are not well enough known; when stretching semicrystalline samples at the same time the original structure deforms, fragments and in some cases starts to melt, whereas at the same time new structural features appear due to reorganization of the free polymer chain segments. Furthermore, as will be discussed below, no unique data treatment for the whole set of samples was possible due to changes in the symmetry of the material.

2. Experimental Section

The HDPE used in this study was supplied by BASELL Polyolefine, Frankfurt, Germany. The molecular weights were $M_w = 3.24 \times 10^5$ g/mol and $M_n = 2.3 \times 10^4$ g/mol. The material was first compression molded at 180 °C and held in the molten state for 5 min. Solidification was induced by rapidly quenching the melt into ice water, yielding a plate of 2 mm thickness. A rectangular strip of 20×70 mm^2 dimension was cut from the plate. The strips were stretched at room temperature until neck propagation occurred at a constant crosshead speed of 10 mm/min. The drawn samples were not fixed at their two ends in the stretched state when taking them out of the tensile machine. The lengths of the samples in the unloaded state were preserved by fixing the samples in metal frames before placing them at the annealing temperatures in a vacuum oven. Samples were annealed at four temperatures (23, 80, 100, and 120 °C) for 24 h. No macroscopic shrinkage was observed during the annealing process. The samples were cooled to room temperature after annealing, and the metal frames were removed before the synchrotron SAXS measurements. In order to measure the strain of the sample along the neck shoulder accurately, optical photo images of the samples were employed. The Hencky measure of the strain ϵ_H was used as a measure for the deformation which is defined as

$$\epsilon_H = 2 \ln \frac{b_0}{b} \qquad (1)$$

where b_0 and b are the widths of the undeformed and deformed area located at certain spots on the samples.
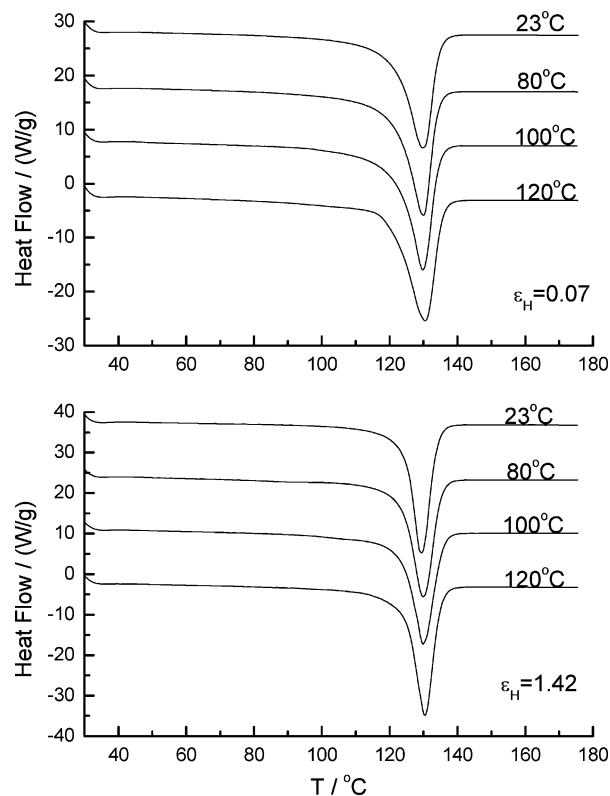

Figure 1. DSC melting curves: samples of the undeformed state (top) and in the necked zone (bottom) after annealing at 23, 80, 100, and 120 °C. Curves were shifted vertically for sake of clarity. Heating rate: 10 K/min.

Synchrotron SAXS measurements were performed at the beamline BW4 at HASYLAB, DESY, Hamburg, Germany. The energy of the X-ray radiation was 8.979 keV, resulting in a wavelength of 0.13808 nm. The size of the primary X-ray beam at the sample position was 0.4×0.4 mm^2. The prestretched sample was mounted onto a 2-dimensional translational stage at the beamline at a sample to detector distance of 3917 mm. At this distance the effective scattering vector q ($q = 4\pi \sin \theta/\lambda$, where 2θ is the scattering angle and λ the wavelength) range is $0.04-0.9$ nm^{-1}. The primary X-ray beam was first positioned at the middle of the horizontally placed sample bar. The samples were then moved stepwise in such a way that the X-ray beam scanned over the neck shoulder at a step length of 0.5 mm, thus covering the stretching ratio from 0.07 to 1.42 on a single sample. SAXS patterns were collected at every step within 60 s. The SAXS data were calibrated for background scattering and normalized with respect to the primary beam intensity. Changes in scattering intensities due to varying sample thicknesses have been corrected for by measuring sample absorption using ionization chambers before and after the sample and performing the respective data correction.

In order to gain more information about the samples, differential scanning calorimetry (DSC) measurements were conducted on samples before and after annealing at two extremes of the draw ratios. A DSC 2920 (TA Instruments) was used during the experiments with a heating rate of 10 K/min. The melting point T_m denotes the minimum of the thermograms during heating. The crystallinity is derived from integrating the DSC traces with respect to a baseline drawn as a tangent to the trace at the temperatures 40 and 150 °C and relating the derived heat to the melting enthalpy of hypothetical 100% crystalline polyethylene of 293J/g.[39]

3. Results and Discussion

3.1. DSC Results. Before considering the structural evolution we present the results from thermal analysis on the polyethylene samples. Figure 1 shows DSC melting curves of samples of un-necked parts and in the neck zones after having been
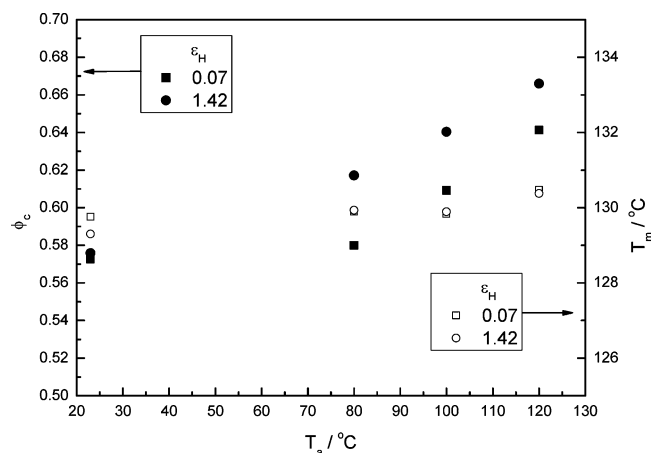
Figure 2. Annealing temperature dependence of crystallinity and melting point of samples before and after deformation.

annealed at different temperatures. Because the plastic deformation set in already before the yield point, the un-necked region of the samples also exhibited several percents of permanent deformation.[40,41] The values of the true strain indicated on the plots of Figure 1 were obtained using eq 1. The melting point and crystallinity values under different conditions are compiled in Figure 2. As seen, annealing hardly affects the melting point. Only a slight increase in the melting point for samples annealed at 120 °C was observed. However, the effect of annealing is expressed more clearly in the values of crystallinity. Two different kinds of behavior were observed for the two types of samples. Although the crystallinity of both samples (un-necked and necked ones) is nearly the same when annealing at room temperature, it shows obvious differences after annealing at elevated temperatures. The crystallinity of the un-necked samples remains unaffected when the annealing temperature is lower than 80 °C. It increased from 58% for samples annealed at room temperature and 80 °C to 64% for the sample annealed at 120 °C. This increase is due to the thickening and perfectioning of the existing crystalline lamellae of the quench-crystallized samples during annealing. It is evident that the samples finished crystallization during quenching at a temperature higher than 80 °C. However, for the samples in the necked zone, a continuous increase in the crystallinity at all annealing temperatures is observed. This is because the crystallites that formed at room temperature during mechanical deformation are no longer stable at temperatures higher than the deformation temperature. The crystallinity for the samples in the necked zone reaches values about 3% larger than those of the un-necked region after being annealed at elevated temperatures from 80 to 120 °C. This is due to the fact that preferential orientation of the crystalline lamellae and polymeric chains in the necked zones facilitates the perfectioning and thickening of the crystallites leading to a higher degree of crystallinity than those in the un-necked regions.

3.2. SAXS Results. Selected SAXS patterns taken at different strains for samples annealed at different temperatures are given in Figure 3. The SAXS patterns for the periodic lamellar structure of HDPE exhibit maxima at q_{max} when scanning along certain directions. The value of the long spacing (d_{ac}) can be calculated using the Bragg equation

$$d_{ac} = \frac{2\pi}{q_{max}} \qquad (2)$$

The long spacing d_{ac} is defined as the average thickness of a lamella together with one interlamellar amorphous layer mea-

sured along the lamella normal. At this point of data treatment we do not take any symmetry considerations into account that might necessitate multiplication of the isotropic intensity values with q^2 (Lorentz correction). We are aware that this leads to an error when comparing the d_{ac} values from isotropic and stretched samples. This point will be addressed in more detail below. As mentioned above, the un-necked region exhibits a permanent macroscopic deformation of $\epsilon_H = 0.07$, which is also evident from the slight anisotropy of the scattering patterns at this deformation. With increasing deformation the SAXS patterns become more anisotropic and finally reach a pattern with two straight streaks perpendicular to the stretching direction at high deformation ratios indicating a highly oriented lamellar structure after deformation. The SAXS patterns for the sample stored at the deformation temperature (23 °C) reflect the microstructural evolution in the deformational process with increasing deformation ratio but without subsequent annealing. In the course of the transition from the original isotropic scattering distribution to highly anisotropic streak-like scattering patterns several features can be identified by closer inspection of the SAXS data.

3.2.1. Sample Annealed at 23 °C. Initially, the original scattering intensity in the meridian direction (i.e., along the stretching direction) becomes weaker with increasing stretching ratio, indicating a loss of the positional correlation between the crystalline lamellae along the stretching direction. Meanwhile, a new meridian long spacing scattering peak appears gradually at larger q values. This finding is in line with the previously proposed fragmentation and recrystallization process during deformation:[22] Since the deformation was imposed at room temperature, the recrystallization process produces lamellae that are thinner than the original ones because of the high undercooling.[42] It should be mentioned that an alternative explanation for this observation was given by Galeski et al. that relies solely on fine-slip and restructuring processes.[21] At the present stage we discuss our data in terms of the fragmentation—recrystallization process since it allows for a consistent interpretation of the results.

In order to investigate the orientational evolution of the original lamellar crystallites we plotted the azimuthal scattering intensity distribution while averaging over a narrow q range ranging from 0.22 to 0.27 nm^{-1} covering the peak of the undeformed sample. Figure 4 gives the results where only one-half of the data is presented for the sake of clarity. Two main features can be identified from the data. First, the normalized scattering intensity decreases strongly with increasing deformation, implying that the original lamellar stacks are destroyed in the course of deformation. This observation can be brought in line with Galeski's fine-slip model when assuming a very disordered fragmented state of the crystals. Second, the azimuthal scattering intensity distribution indicates a four-point SAXS pattern at small deformation ($\epsilon_H = 0.17$) at angles close to 45° with respect to the stretching direction. The positions of these peaks move closer to the equator. These observations can be tentatively explained in the following way. First, lamellae with their normal parallel to the stretching direction are molten or broken into blocks or fragments losing their positional correlation because they cannot easily undergo slip-like deformation. This point was already addressed above. Second, lamellae with their normal perpendicular to the stretching direction are broken by external forces resulting in a loss of SAXS intensity in the equatorial direction. Third, lamellar stacks with their normal situated between the above two extremes are able to experience intralamellar slip, keeping some correlation within the stacks. The decrease in SAXS intensity indicates that
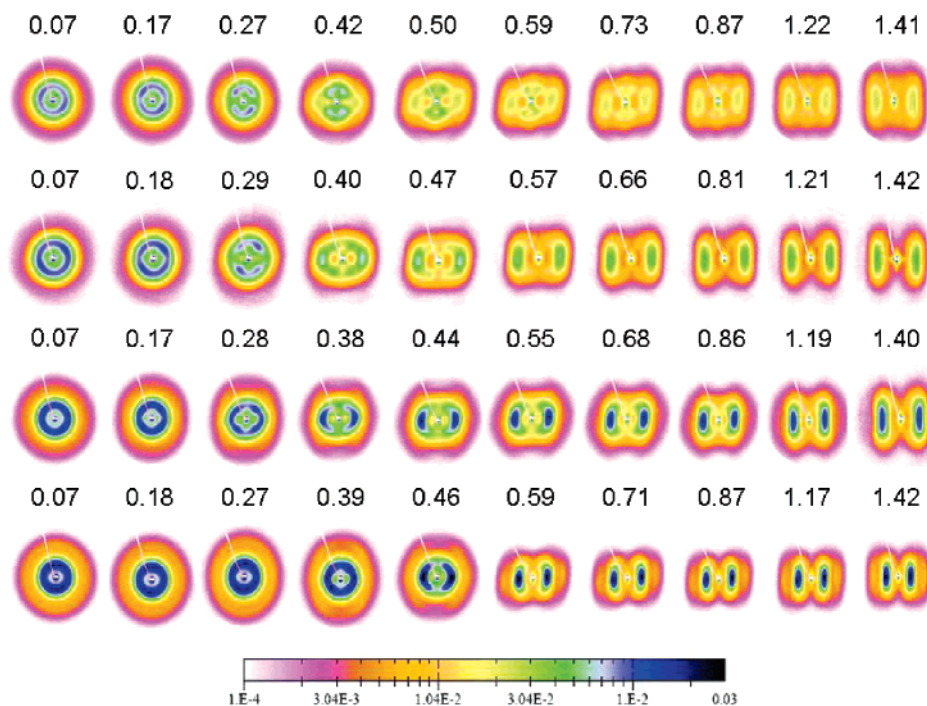
Figure 3. Selected small-angle X-ray scattering patterns of uniaxially drawn quenched PE followed by annealing at 23, 80, 100, and 120 °C (from top to bottom) taken at different strains as indicated on the graph. Stretching direction: horizontal.
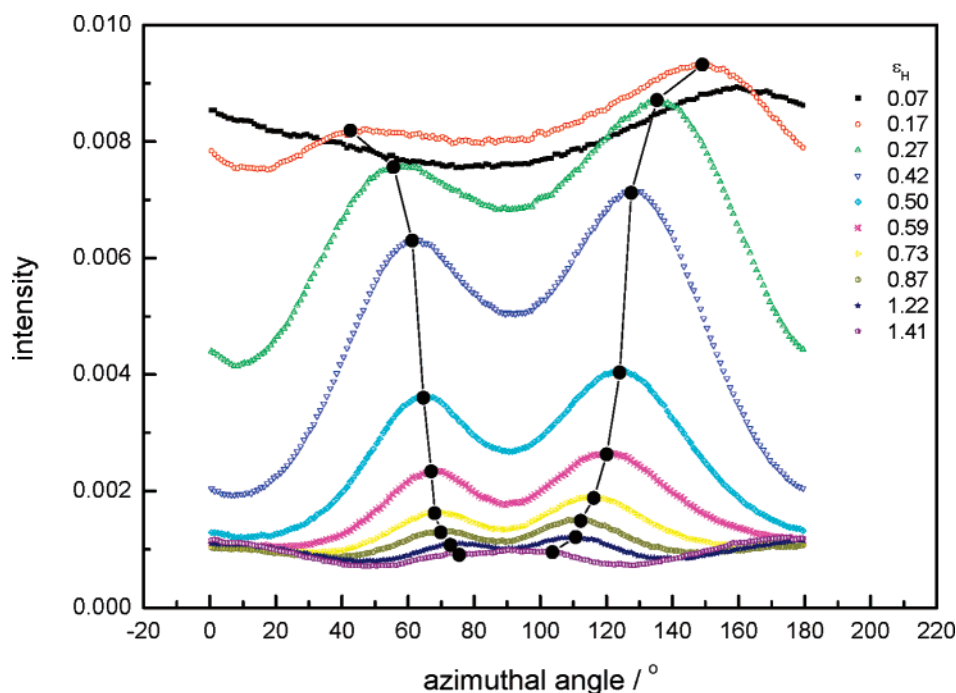

Figure 4. Sample annealed at 23 °C: Azimuthal intensity distributions of the scattering intensity of the original lamellar long spacing. The q range (from 0.22 to 0.27 nm^{-1}) covers the SAXS peak of the undeformed sample. The data sets are not shifted but plotted to scale with the same baseline.

the original lamellar structure is destroyed gradually during deformation. Alternatively to the foregoing discussion one might also consider the possibility of kinking deformation of lamellae as proposed by Bartczak and Lezak, which also produces four-point patterns in SAXS.[16] We cannot exclude this possibility, but given the drastic decrease of intensity during deformation it seems safer to assume that the crystals break and loose their correlation.

3.2.2. Samples Annealed at Elevated Temperatures. The effect of annealing on the SAXS patterns and thus the microstructure of samples is also derived from the data in Figure 3. First, there is an overall increase in the scattering intensity after annealing which is evidence for the perfection of crystalline lamellae accompanied by an increase of the electron density difference between the crystalline lamellae and the amorphous layers in between. Second, the position of the maximum scattering intensity moved to smaller q values after annealing, implying that the crystalline lamellar long spacing increased. Finally, at small and very large deformations no qualitative differences of the shape of the SAXS patterns were observed with respect to the annealing temperature, whereas at moderate deformations the SAXS patterns change their intensity distribution strongly (patterns at strains around 0.5).
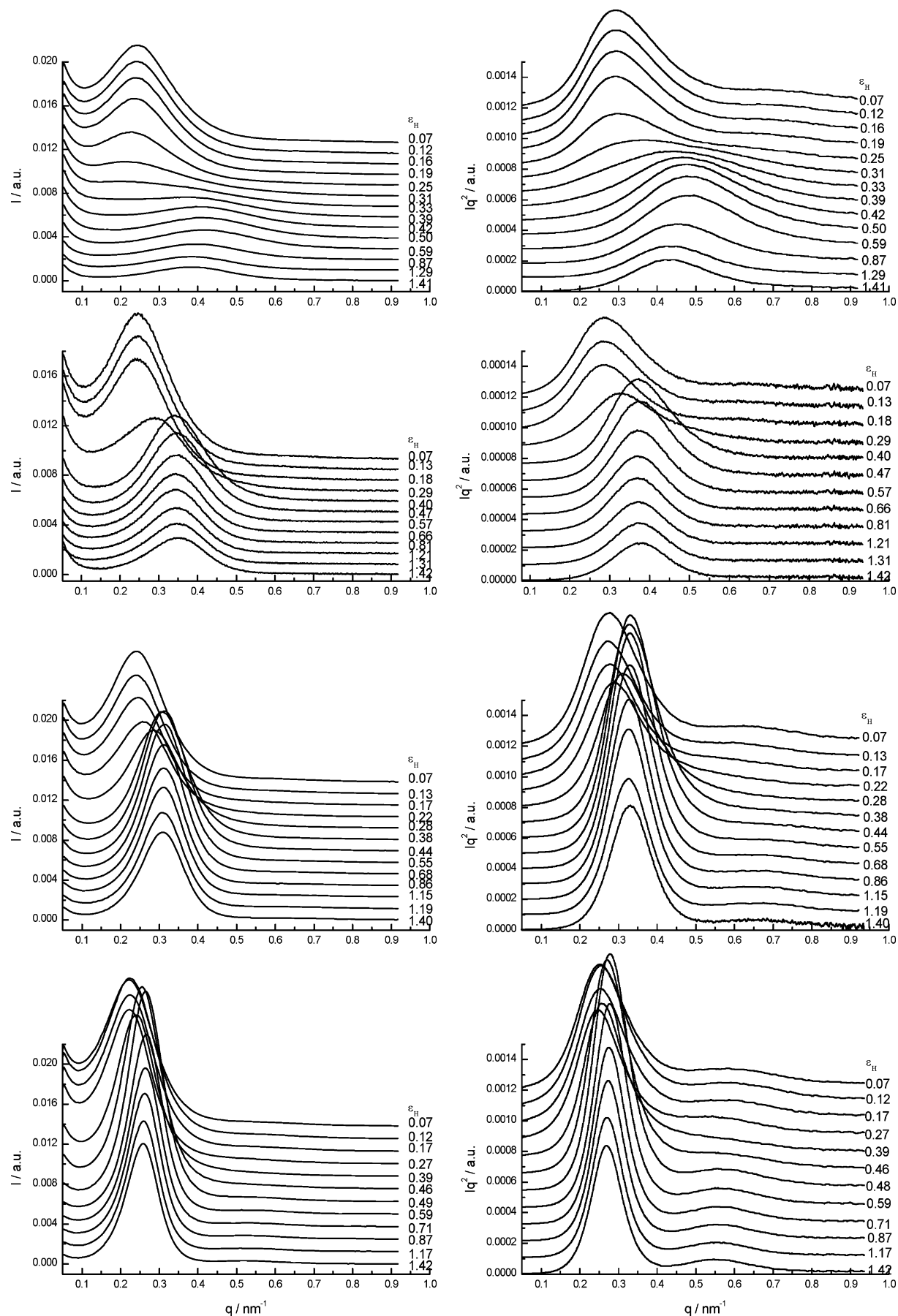
Figure 5. Plots of *I* vs *q* (left) and Iq^2 vs *q* (right) along the stretching direction at different deformations for samples annealed at 23, 80, 100, and 120 °C (from top to bottom). Peak positions were used to calculate the long periods (d_{ac}).
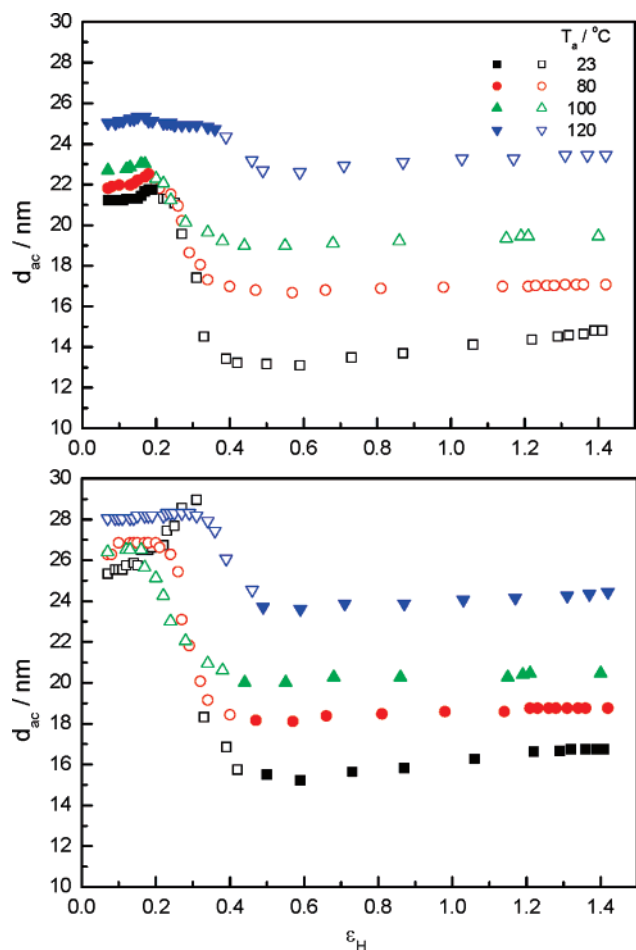
Figure 6. True-strain dependence of the long period d_{ac} along the drawing direction at different annealing temperatures. (Top) Data derived from Lorentz-corrected scattering curves; filled symbols represent regions where Lorentz correction can safely be applied. (Bottom) Data derived from scattering curves without Lorentz correction; filled symbols stand for regions where anisotropy is high enough such that no Lorentz correction must be applied.

In an effort to elucidate the evolution of the lamellar long spacing after deformation and annealing, the one-dimensional scattering intensity distributions along the stretching direction are plotted in Figures 5. We took two approaches: in order to represent the data of the isotropic samples with the correct q weighting the scattering intensity was multiplied by q^2 for data processing (Lorentz correction).[43] For the data with fiber symmetry, i.e., at high stretching rations, no Lorentz correction was applied. Both sets of data are represented in Figure 5. Obviously, both approaches are correct only for the respective extreme situations where the lamellar stacks are distributed isotropically, i.e., sample without strain, and stacks of lamellae perfectly oriented along the drawing direction. In between no unique recipe for data treatment can be given because of the uneven distribution of scattered intensity in reciprocal space. The long spacing values for samples after deformation and annealing measured along the stretching direction were obtained according to eq 2 for both data sets in Figure 5 and are given in Figure 6. The data show that although the long spacings derived from Lorentz-corrected data at small strains show few nanometers difference from the respective long spacings derived from the uncorrected data, it does not change the characteristic variation of the long spacing as a function of strain. That means that for a semiquantitative discussion of the dependence of the long spacing on strain the type of data treatment (Lorentz correction or not) plays only a subordinate role. Development

of new lamellar long spacing peaks along the stretching direction at larger q values after deformation is clearly seen in Figure 5. Figure 6 shows that the variations of the long spacing values along the stretching direction with strain exhibit a transition-like behavior. For the sample annealed at room temperature there exists a large long spacing jump from about 21 nm before necking to around 15 nm in the necked zone. This behavior is assumed to be due to the fragmentation and recrystallization process during deformation; an alternative explanation based on the fine-slip model is given below. The transitional strain lies between 0.3 and 0.4; this is in accordance with previous results obtained using true stress−strain experiments.[28] A closer look reveals that the long spacing along the stretching direction increases slightly both before and after the transition zone. This can be interpreted by assuming that under external tensile stress in those lamellar stacks with their normal parallel to the stretching direction the interlamellar amorphous layers are stretched. Figure 6 shows that annealing leads to an increase of the long spacing in the drawing direction. When the annealing temperature is lower than 100 °C, the long spacing follows essentially the above trend through the transitional strain zone where a drastic decrease of the long spacing occurs which then remains almost constant. The only difference between the samples annealed at 80 and 100 °C is the amount of increase of the long spacing compared to the value measured at the 23 °C sample at corresponding strains with annealing temperature.

When the sample was annealed at 120 °C, in addition to the further increase of the long spacing as compared to that at lower annealing temperatures, one finds a two-step change of the long spacing with strain. In the first step—between ϵ_H values of 0.1 and 0.3—only a slight decrease of the long spacing occurs at about the same position as the step-like decrease of d_{ac} of the samples annealed at lower temperatures, whereas the second step occurs at higher strains. More information can be extracted from the 2-dimensional SAXS patterns in Figure 3. As soon as the new lamellar stacks along the stretching direction have been established at a strain of about 0.4, cf. Figure 6, the four-point patterns of the original lamellar stacks, compare data of 23 °C sample, are not stable when annealing. Although the lamellar stacks established after stretching have far smaller long spacing and thinner lamellae than the original ones, they are more stable during annealing; they obviously take up the polymer chain segments freed from destabilized original crystalline lamellae that have been destroyed during deformation. The original tilted lamellae are destabilized by intralamellar block-slip processes; they are even not stable at the annealing temperature of 80 °C, cf. Figure 3. At moderate deformation the newly developed lamellae with their normal parallel to the stretching direction act as nuclei at the lower annealing temperatures of 80 and 100 °C, where the original lamellae melted and recrystallized. However, when the annealing temperature is raised to 120 °C, at moderate strains, most of the newly developed lamellae melt together with most of the original destabilized ones and recrystallize in an isotropic fashion onto residual crystal fragments. Because of the increased stability with strain of the newly developed lamellae the anisotropic lamellae are retained above a certain strain and serve as nuclei. Therefore, we observe a two-step decrease of the lamellar long spacing along the stretching direction. We are aware that two competing models are used to describe observations such as the ones given in this paper. On one hand, we argue in favor of a block-slip, fragmentation, and recrystallization sequence, whereas Galeski et al. bring arguments in favor of a fine-slip, break-up or coarse

chain slip, pinch-off, restructuring sequence, cf. their Figure 22 in ref 21. We think that both approaches can be unified at least to a certain degree: the fragmentation we are referring to does not always have to imply that the original crystal is completely molten, meaning that locally the chain segments are isotropically distributed. Rather it might be assumed that locally orientational correlation between bundles of chain segments is retained or that even small fragments of blocks remain, similar to what is depicted in Figure 22e of ref 21. This discussion of course does not affect the foregoing considerations about the annealing effects where it was shown in the past unequivocally that local fragmentation and recrystallization occurs.

4. Conclusions

In summary, our scanning synchrotron SAXS experiments support previous reasoning about the deformation mechanism of semicrystalline polymers where a stress-induced fragmentation and recrystallization process occurring at a certain strain was postulated. Moreover, the effect of annealing on samples deformed to different strains was investigated. It was found that the most pronounced effect of annealing on the microstructure of a deformed HDPE is observed at moderate strains where the fragmentation and recrystallization process started. Although the newly formed lamellar crystallites with their normal along the stretching direction have a smaller long period, they are more stable than the deformed original crystalline lamellae. When the annealing temperature is lower than 100 °C, the newly developed lamellae serve as nuclei so that the original lamellae melt and recrystallize onto them, forming thicker lamellar crystals with the normal along the stretching direction. However, the newly developed lamellae also have a certain stability limit as evidenced by the SAXS results on the sample annealed at 120 °C where these thinner lamellae also melted resulting in a nearly isotropic scattering pattern at intermediate strains.

References and Notes

(1) Bartczak, Z. *Macromolecules* **2005**, *38*, 7702.
(2) Failla, M. D.; Mandelkern, L. *Macromolecules* **1993**, *26*, 7167.
(3) Kennedy, M. A.; Peacock, A. J.; Mandelkern, L. *Macromolecules* **1994**, *27*, 5297.
(4) Kiass, N.; Khelif, R.; Boulanouar, L.; Chaoui, K. *J. Appl. Polym. Sci.* **2005**, *97*, 272.
(5) Strobl, G. *The Physics of Polymers,* 2nd ed.; Springer: Berlin, Germany, 1997.
(6) Men, Y.; Strobl, G. *J. Macromol. Sci., Phys.* **2001**, *B40*, 775.
(7) Men, Y. F.; Rieger, J.; Strobl, G. *Phys. Rev. Lett.* **2003**, *91*, 095502.
(8) Butler, M. F.; Donald, A. M.; Bras, W.; Mant, G. R.; Derbyshire, G. E.; Ryan, A. J. *Macromolecules* **1995**, *28*, 6383.
(9) Hughes, D. J.; Mahendrasingam, A.; Heeley, E. L.; Oatway, W. B.; Martin, C.; Towns-Andrews, E.; Fuller, W. *J. Synchrotron Radiat.* **1996**, *3*, 84.
(10) Pawlak, A.; Galeski, A. *Macromolecules* **2005**, *38*, 9688.
(11) Ran, S. F.; Wang, Z. G.; Burger, C.; Chu, B.; Hsiao, B. S. *Macromolecules* **2002**, *35*, 10102.
(12) Men, Y.; Strobl, G. *Chin. J. Polym. Sci.* **2002**, *20*, 161.
(13) Young, P.; Stein, R. S.; Kyu, T. *J. Polym. Sci. Polym. Phys.* **1990**, *28*, 1791.
(14) Song, H. H.; Argon, A. S.; Cohen, R. E. *Macromolecules* **1990**, *23*, 870.
(15) Gerrits, N. S. J. A.; Tervoort, Y. *J. Mater. Sci.* **1992**, *27*, 1385.
(16) Bartczak, Z.; Lezak, E. *Polymer* **2005**, *46*, 6050.
(17) Bowden, P. B.; Young, R. J. *J. Mater. Sci* **1974**, *9*, 2034.
(18) Peterlin, A. *J. Mater. Sci.* **1971**, *6*, 490.
(19) Young, R. J.; Bowden, P. B.; Ritchie, J. M.; Rider, J. G. *J. Mater. Sci.* **1973**, *8*, 23.
(20) Schultz, J. M. *Polymer Materials Science;* Academic Press: Englewood Cliffs, NJ, 1974.
(21) Galeski, A.; Bartczak, Z.; Argon, A. S.; Cohen, R. E. *Macromolecules* **1992**, *25*, 5705.
(22) Flory, P. J.; Yoon, D. Y. *Nature* **1978**, *272*, 226.
(23) Wu, W.; Wignal, G. D.; Mandelkern, L. *Polymer* **1992**, *33*, 4137.
(24) Keller, A.; Pope, D. P. *J. Mater. Sci.* **1971**, *6*, 453.
(25) Peterlin, A.; Meinel, G. *Makromol. Chem.* **1971**, *142*, 227.
(26) Meinel, G.; Peterlin, A. *Colloid Polym. Sci.* **1970**, *242*, 1151.
(27) Corneliussen, R.; Peterlin, A. *Makromol. Chem.* **1967**, *105*, 193.
(28) Hiss, R.; Hobeika, S.; Lynn, C.; Strobl, G. *Macromolecules* **1999**, *32*, 4390.
(29) Butler, M. F.; Donald, A. M.; Ryan, A. *Polymer* **1997**, *38*, 5521.
(30) Liu, L. Z.; Hsiao, B. S.; Fu, B. X.; Ran, S. F.; Toki, S.; Chu, B.; Tsou, A. H.; Agarwal, P. K. *Macromolecules* **2003**, *36*, 1920.
(31) Kasal, N.; Kakudo, M. *J. Polym. Sci., Part A* **1964**, *2*, 1955.
(32) Hay, I. L.; Keller, A. *J. Mater. Sci.* **1967**, *2*, 538.
(33) Cowking, A.; Rider, J. G.; Hay, I. L.; Keller, A. *J. Mater. Sci.* **1968**, *3*, 646.
(34) Fleissner, M. *Kunststoffe* **1987**, *77*, 45.
(35) Fischer, E. W.; Schmidt, G. F. *Angew. Chem., Int. Ed.* **1962**, *1*, 488.
(36) Peterlin, A.; Corneliussen, R. *J. Polym. Sci., Part A-2* **1968**, *6*, 1273.
(37) Men, Y. F.; Rieger, J.; Lindner, P.; Enderle, H.-F.; Lilge, D.; Kristen, M. O.; Mihan, S.; Jiang, S. C. *J. Phys. Chem. B* **2005**, *109*, 16650.
(38) Yeh, G. S. Y.; Hosemann, R. *Polymer* **1976**, *17*, 309.
(39) Wunderlich, B. *Macromolecular Physics;* Academic Press: New York, 1973; Vol. 1.
(40) Hobeika, S.; Men, Y.; Strobl, G. *Macromolecules* **2000**, *33*, 1827.
(41) Al-Hussein, M.; Strobl, G. *Macromolecules* **2002**, *35*, 8515.
(42) Peterlin, A.; Balta-Calleja, F. J. *Kolloid-Z. Z. Polym* **1970**, *242*, 1093.
(43) Glatter, O.; Kratky, O. *Small-Angle X-ray Scattering;* Academic Press: London, U.K., 1982.